Experimental tests of an in-situ oceanic radiation monitoring prototype system

Seungeun Lee[a], Jae Sung Lee[a], Han Soo Kim[b], Jeongmin Park[b], Seungjae Baek[c], Yujae Song[c], Jung-min Seo[c], Soo Mee Kim[c*]
[a]*Department of Biomedical Sciences, Seoul National University, Seoul, Korea*
[b]*Advanced Radiation Technology Institute, Korea Atomic Energy Research Institute, Jeongup, Korea*
[c]*Maritime ICT R&D Center, Korea Institute of Ocean Science and Technology, Busan, Korea*
[*]*Corresponding author: smeekim@kiost.ac.kr*

1. Introduction

Importance of daily radiation monitoring system has been emphasized in terms of radiation protection because of growing number of nuclear power plants in the neighbor countries and existing potential hazard of nuclear reactor accidents involving radiation leakage. Korean environmental radiation monitoring service, IERNet (integrated environmental radiation monitoring network) [1] updated every three months by sampling sea water of 60 kg at 21 oceanic spots and analyzing the radio-activities in the laboratory. For the fast and accurate periodic radiation monitoring, the on-site radiation detection is essential. We developed a prototype system of unmanned surface vehicle (USV) carrying radiation sensor (CsI(Tl) crystal + PIN diode) to measure real-time oceanic radiation level of desired regions from coast to deep sea. In this study, we experimented the detectability of the system and compared the results with simulation data. We targeted on detecting 662 keV gamma ray emitted by ^{137}Cs, which is a major fission product.

2. Methods and Results

2.1 System description

A radiation sensor consisted of $10\times10\times20$ mm^3 CsI(Tl) scintillation crystal, silicon PIN diode, and built-in electronic circuits with amplifiers and data acquisition system. The energy resolution of the sensor was 22% in full width half maximum (FWHM) at 662 keV. We used a multichannel analyzer (MCA; EASY-MCA-2k, ORTEC) to measure an energy spectrum of detected radiation. The MCA was connected to a USB-over-IP hub to transfer the measured digital data to a remote laboratory PC.

Fig 1. Overall configuration of the in-situ oceanic radiation monitoring system.

Besides the radiation sensor part, battery, sonar imaging system, and communication system are located inside FRP-carbon body of the USV. Movement of the USV was controlled by a remote controller or predefined path. Real-time position information of the USV was recorded by global positioning system.

2.2 Simulation

We used Geant4-based GATE Monte Carlo simulation toolkit (v7.0) [2] to predict detection efficiency of the system. The USV was simplified as a $170\times38\times28$ cm^3 box with 1 cm thickness and density of 1.9 g/cm^3. The size of CsI(Tl) crystal was $10\times10\times20$ mm^3, and the density was 4.51 g/cm^3. As shown in Fig 2, the crystal was located inside the USV, and the USV was placed on the surface of $1500\times1000\times600$ cm^3 water tank with the bottom half sunk. The ^{137}Cs ion point source was placed with 0-200 cm distant from the USV. The activity of the source was 83 μCi, and the acquisition time at each distance was 5 minutes.

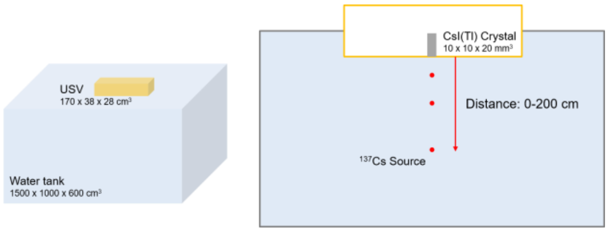

Fig 2. Monte Carlo simulation setup.

The total decay number of the ^{137}Cs source during the acquisition time was 9.21×10^8. We measured the count number of detected 662-keV gamma rays and the scatter fraction which is a ratio of the events underwent one or more Compton scatters before detection among the total detected events. We tested two different energy windows of [520, 800] keV and [590, 735] keV which were the windows around 662 keV with the widths corresponding to 1 and 2 times of FWHM of the system energy resolution, respectively.

As shown in Fig 3(a), the longer distance between the crystal and the source resulted in lower sensitivity because a large proportion of gamma rays were attenuated by USV carbon body and water. Fig 3(b) shows that at 0 cm distance, 60% of the detected gamma rays underwent Compton scatters in USV body, while water contributes more largely in longer distance. Additionally, cross-sectional area of the crystal facing the source was inversely proportional to the square of the distance, which led to lower geometric detection efficiency. The results at 200 cm are not shown because no event was detected.

By applying narrower energy window, less events were counted because a large amount of events was rejected (Fig 3(a)). However, scatter fraction was lower, which indicates that narrow energy window effectively rejects the Compton-scattered 662-keV gamma rays (Fig 3(b)).

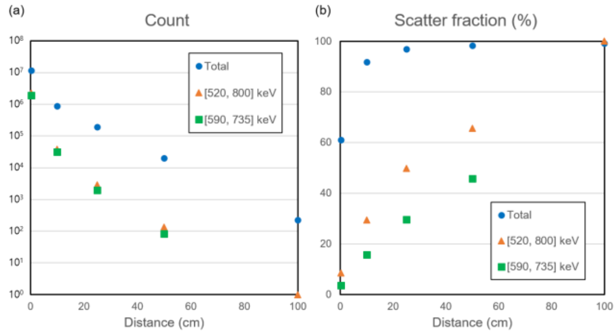

Fig 3. Simulation results. (a) Detected count and (b) scatter fraction at various distances between the USV and the source with applying different energy windows.

2.3 Water tank experiment

We performed an experiment inside a water tank facilitated in UTEC. The radiation sensor and the MCA were wrapped with aluminum foil to shield interference between the cables (Fig 4(a)). The USV floated on the center of the water tank without movement (Fig 4(b)). We firstly obtained the background data without any radioactive source inside the water tank. The 83 μCi ^{137}Cs point source was tied to a rope with 0, 10, 25, 50, 100, and 200 cm distant from the bottom of the USV. To test another activity, we additionally put the source in a lead case and measured the count rate with a dosimeter. The equivalent activity of the source inside the case was approximately 1/3 of the original activity. The data acquisition time was 5 minutes for each activity and distance setup. We counted the events applying an energy window of [520, 800] keV around the pre-calibrated 662-keV peak.

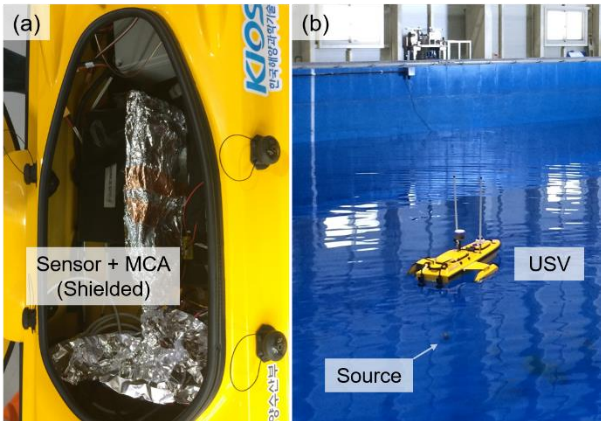

Fig 4. Water tank experiment setup. (a) Radiation sensor positioned inside the USV body. (b) USV in the water tank with source tied in certain distance.

Fig 5 shows the background energy spectrums when the USV is placed inside and outside the water tank without any source. For both spectrums in common, background noise was concentrated in low energy bins (< 300 keV) because of intrinsic noise contributed by the sensor and analog-to-digital converter in the MCA. However, the noise was insignificant around 662 keV region. The count of noise within the energy window of [520, 800] keV was 18, and it was subtracted from the measured counts from hence in the experiment.

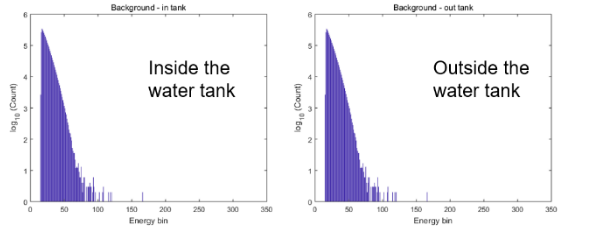

Fig 5. Background energy spectrum with USV located inside and outside the water tank. The counts are shown in log scale.

Fig 6 shows the measured energy spectrums with varying the distance between the USV and the point source under the water. When the source was located farther, the count decreased and the 662-keV peak was more undistinguishable. The peak was distinguishable when the distance was shorter than 50 cm, while the spectrums were almost identical to the background spectrum when the distance was longer than 100 cm.

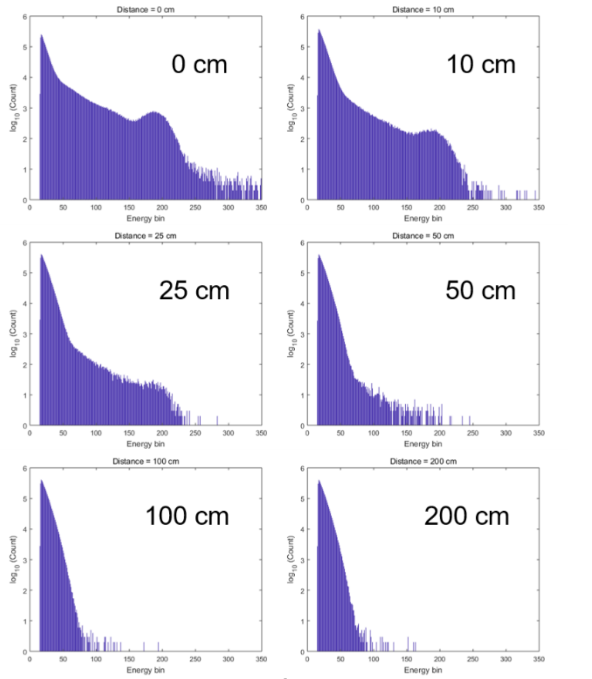

Fig 6. Energy spectrums of ^{137}Cs source located in different distances from the bottom of the USV without background count subtraction. The counts are shown in log scale.

The detected count ratio between source located outside and inside the lead case were consistently near 3, which was similar to activity ratio as mentioned in the section 2.3 (Fig 7). However, when the distance was longer than 50 cm, count ratios are meaningless because 662-keV peaks were rarely visible in energy spectrums in Fig 6 and the statistical noise counts were dominant. Therefore, the linearity between the detected counts and activity was preserved only when significant number of events was detected under the peak region in the energy spectrum.

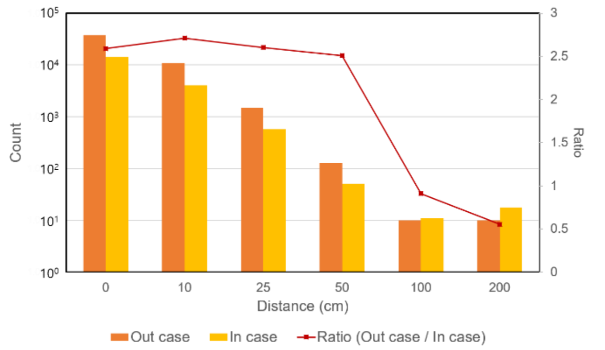

Fig 7. Detected counts and count ratio when source was placed outside and inside the lead case. The applied energy window was [520, 800] keV and the background counts were subtracted.

Comparison of the simulation and experiment results is shown in Table 1. The difference was considerable especially at 0 cm because there were several unideal factors which were not considered in the simulation setup. First, in the experiment, electronic equipment and shielding materials contributed to attenuation of the gamma rays. In addition, error of relative position of the source to the sensor existed in reality. The effect of attenuation and position error reduced when the distance was longer. Second, limitation in detection efficiency of the PIN diode in radiation sensor is also one of the possible reasons why less count was detected, while the efficiency was assumed to be 100% in simulation. Lastly, simulation could not reflect the noise property of the system because the sensor and MCA were highly vulnerable to noise in spite of electromagnetic shielding. Data at the distances longer than 50 cm were meaningless because only noise was counted in the experiment.

With Monte Carlo simulation, we could predict rough range of distance where the gamma ray from the ^{137}Cs source would be significantly detected. However, we could not show the reliability of simulation on detected counts. To obtain reliable expected results from the simulation, the unideal factors mentioned above need to be intensely reflected to the simulation setup and electronics robust to noise will be implemented in the future study.

Table 1. Comparison of experiment and simulation results. The applied energy window was [520, 800] keV commonly.

Distance (cm)	Count (Experiment)	Count (Simulation)	Ratio (Experiment / Simulation)
0	37232	2258662	0.0165
10	10911	38122	0.286
25	1504	2854	0.527
50	128	134	0.955
100	10	1	10
200	10	0	-

3. Conclusions

We conducted an initial experiment of our newly developed in-situ ocean radiation monitoring system with varying the ^{137}Cs source position. The results demonstrated that the system is able to detect 662-keV gamma rays of underwater ^{137}Cs source with depth less than 50 cm, and showed the linearity between the count and the activity of the source. With Monte Carlo simulation, we could expect the tendency of the results but further substantial modification of setup is required. In future work, we will measure the background radiation level in the real coast. To improve the sensitivity of the system, using the radiation sensor with larger cross-section and better energy resolution and robustness to noise are considered.

ACKNOWLEDGEMENT

This work was supported by research grants from Korea Institute of Ocean Science and Technology (PE99672). Also, this research was a part of the project titled 'Development on technology for offshore waste final disposal', funded by the Ministry of Oceans and Fisheries, Korea. Specially thanks to supporting radiation sensors from radiation equipment fab. center in KAERI.

REFERENCES

[1] IERNet, http://iernet.kins.re.kr/
[2] S Jan et al., GATE a simulation toolkit for PET and SPECT, Physics in Medicine and Biology, Vol. 49, No. 19, 2004.